Electron Density Topological Properties Are Useful To Assess the Difference between Hydrogen and Dihydrogen Complexes

David Hugas, Sílvia Simon,* and Miquel Duran

Institut de Química Computacional and Departament de Química, Universitat de Girona, 17071-Girona, Catalonia, Spain

Received: January 5, 2007; In Final Form: March 14, 2007

B3LYP/6-31++G(d,p) and MP2/6-31++G(d,p) calculations for a series of hydrogen- and dihydrogen-bonded systems have been carried out in order to analyze the topology of the electron density and the energy densities at the respective energy-optimized bond critical points. Even though there are no significant differences when these properties are represented as a function of the dimerization energy, they can be separated into two well-defined sets if those properties are correlated with intermolecular distances. When analyzing the dependence of various properties with equilibrium bond lengths, the specific trends of dihydrogen bond systems consist of (a) lower electron density at the bond critical point, and (b) lower concentration/depletion of that density which can be translated in a different behavior for the Laplacian components. Furthermore, the sets of molecules form two different plots which allow for a valuable classification between hydrogen- and dihydrogen-bonded systems.

I. Introduction

Hydrogen-bonded (HB) systems have become of utmost importance in chemistry and biology, their theoretical study having received a great deal of attention during recent decades.[1] Dihydrogen-bonded systems, a new, particular case of hydrogen-bonded complexes, have recently acquired special attention through a number of theoretical and experimental studies.[2−4] Although classical hydrogen bonds (A−H···B) are formed between an acidic hydrogen and a proton acceptor, if this proton acceptor consists of a molecule with a hydrogen atom as the acceptor, then a dihydrogen bond (DHB) is built. Indeed, this type of weak interaction between hydrogen atoms emerges when they bear charges of different signs; those charges may be induced by electronegative or electropositive neighboring atoms. The dihydrogen bond can be represented as X−H···H−M, where M stands for an element which is less electropositive than hydrogen (e.g., transition metals, Li, Be, B, ...) and X stands for a conventional electronegative element or group.

Hydrogen bonds (and intermolecular interactions in general) can be classified using energetic or geometrical criteria. For instance, topological characterization of the electron density $\rho(r)$ in the intermolecular regions allows for an accurate analysis based on quantitative interpretation of the electron density distribution, its Laplacian, and its principal curvatures at the bond critical points (bcp). Nowadays, such a topological analysis is one of the most useful tools to characterize atomic and molecular interactions; thus, many studies of hydrogen bonding from the point of view of the Atoms in Molecules theory[5] (AIM) can be found in the literature. In particular, Koch and Popelier[6] have proposed a set of topological criteria that a bond must fulfill in order to be considered as a hydrogen bond; such criteria were applied to classify the dihydrogen-bonded interaction.[7]

Among all topological properties used to analyze the electron density, energetic properties of the electron density distribution at the bond critical point ($G(r_{bcp})$ and $V(r_{bcp})$) are quite useful to assess the character of the bond. For instance, Espinosa et al.[8] have discussed the relationship between the principal curvatures of $\rho(r)$ at the bcp and the energetic properties of $\rho(r_{bcp})$, $G(r_{bcp})$, and $V(r_{bcp})$, thus leading to a new representation of the topological characteristics of electron density in terms of those properties of $\rho(r)$ and vice versa. Furthermore, the same authors have tried to classify hydrogen bonds using topological and energetic properties of intermolecular bcp derived from experimental electron densities.[9] In another study, Grabowski has used the AIM theory as a measure of hydrogen-bonding strength in conventional and unconventional hydrogen bonds.[10,11] Moreover, the electron localization function (ELF) has been used to established topological criteria to distinguish between weak, medium, and strong hydrogen bonds.[12]

Recently, very strong hydrogen-bonded systems have deserved increased attention. One can find in the literature different studies of the covalent contribution to this very short hydrogen bond. Espinosa et al. studied the X−H···F−Y interaction by performing a comprehensive analysis of the intermolecular topology and energetic properties of $\rho(r)$ from weak to strong hydrogen bonds.[13] Their conclusions were supported by Gálvez et al.,[14] who analyzed different intermolecular interactions. Espinosa et al. classified weak and strong hydrogen bonds from pure closed-shell interactions (weak interaction) to pure shared-shell interaction (very strong HB), including various levels of contribution of covalent character. Pacios[15] claimed that topological indices cannot be used to identify equilibrium structures, because their change with intermolecular distances does not show special trends. Concerning dihydrogen-bonded systems, some theoretical and experimental studies have recently appeared, where very short H···H distances have been reported,[17,18] mainly related to a dehydrogenation reaction. Grabowski et al.[20] studied, in the framework of AIM theory and energy decomposition analysis, how short the dihydrogen intermolecular distance contact may be, concluding that very short H···H intermolecular distances are partly covalent.

Very recently, $CH^{\delta+}\cdots{}^{\delta+}HC$, CH···O, and CH···C weak interactions in three organic crystals have been compared by

* Corresponding author. E-mail: silvia.simon@udg.es.

10.1021/jp070080u CCC: $37.00
Published on Web 04/25/2007

analyzing experimental densities at the H···H and hydrogen bond critical points.[21] This study stresses also the importance of the assessment of the bond type to understand the conformation of molecules in their crystalline state and their stability.

Indeed, dihydrogen bonds and hydrogen bonds share a common trend; however, dihydrogen bonds are very particular because a bond is formed between two very particular atoms—hydrogens. This special bond has received the focus of earlier studies, especially on the relationship between topological parameters and energetic properties of $\rho(r_{bcp})$; furthermore, their studies have not assessed clearly enough the different trends shown between dihydrogen-bonded systems and other hydrogen-bonded complexes when geometric parameters are considered. Moreover, the above-mentioned study[21] on the relationship between H···H electron density at the bond critical point and hydrogen bond length is limited to a few, particular, organic interactions.

In previous papers of our group, we have reported some general studies of dihydrogen-bonded systems and analyzed them using the AIM theory; the aim of the present paper is to complement these earlier studies on differences between hydrogen- and dihydrogen-bonded systems, focusing especially on the dependence of density parameters with geometries, while dealing with complexes ranging from weak to very strong. For this purpose, the intermolecular electron density, its Laplacian, and also its components at the bond critical point (and optimized equilibrium geometry) will be analyzed. This analysis will be performed first as a function of the hydrogen/dihydrogen equilibrium bond length and later as a function of the interaction energy as a measure of intermolecular strength in order to assess which parameters are the most suitable to separate HB and DHB interactions.

II. Computational Details

For all monomers and dimers considered in this study, molecular geometries were optimized at the nonlocal three-parameter hybrid B3LYP and at the MP2 levels of theory.[22] MP2 is one of the most economical post-Hartree−Fock methods that account for the full range of intermolecular interactions: electrostatic, induction, and dispersion effects. Even though the B3LYP approach does not account for dispersion interactions, several studies have shown a reasonably good performance of DFT methods.[19(a)] In order to check DFT results, a comparison of both methods will be discussed in the next section. MP2 calculations were performed correlating all the electrons except the inner shells.

The 6-31++G(d,p) basis set was chosen for being one of the most popular basis sets used in the study of medium- and large-sized hydrogen-bonded systems as well as for yielding a very small BSSE[23] with countepoise-corrected values comparable to those of the larger 6-311++G(3df,2pd) basis set. The countepoise correction (CP) proposed by Boys and Bernardi[24] has been calculated to the dimerization and interaction energies in order to compare MP2 and B3LYP energetic data. Vibrational analyses of optimized systems show that their structures are always a minimum on the potential energy surface, except for XH···HM (M = Li,Na).[18] The latter systems exhibit a double degenerate imaginary frequency which corresponds to the formation of H_2. All calculations were carried out with the Gaussian 03 package.[25]

Bond critical points were characterized using the AIM2000 program[26] based on Bader's Atoms in Molecules Theory. The electron density and its Laplacian were obtained for each intermolecular interaction, as well as the kinetic and potential energy densities ($G(r_{bcp})$ and $V(r_{bcp})$, respectively) evaluated at the bcp.

CHART 1: Molecular Structure of the Dimers[a]

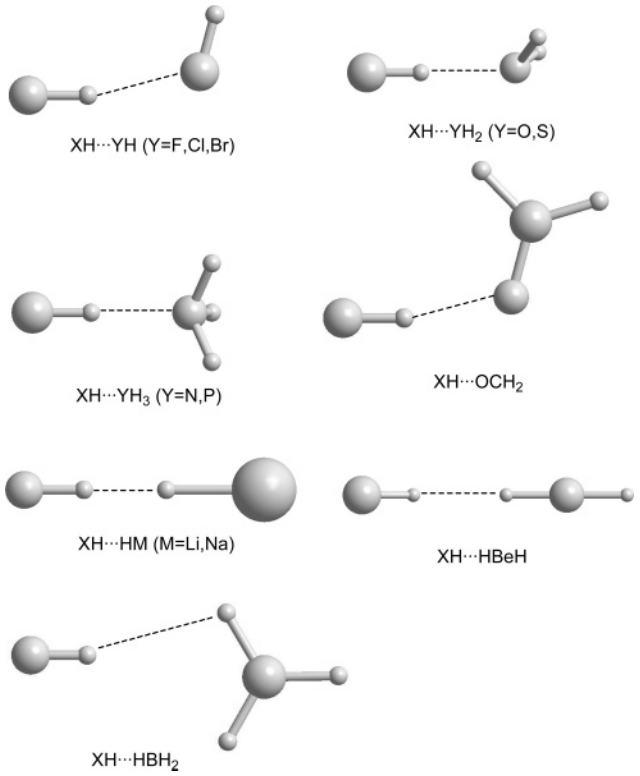

[a] Geometrical parameters can be found in refs 4, 18, and 19 and in Table S.1 in Supporting Information.

III. Results

In Chart 1 we depict the structure of all different dimers studied in this paper and how they are bonded. In all cases, hydrogen halides (H−X, where X = F, Cl, Br) were used as proton donor, while seven different atoms or groups were chosen as proton acceptors. As pointed out above, when the proton acceptor is a hydrogen atom, the interaction is defined as a dihydrogen bond.

Tables 1 and 2 collect all the energetic, geometric and topological data of the various complexes considered in the present study at the B3LYP and MP2 levels of theory, respectively. Interaction energies (E_{int}, in kcal/mol) correspond to the dimer formation taking into account the nuclear relaxation of each monomer (i.e., to D_e, the difference between the absolute energy of the minimum and separate, optimized monomers) while the dimerization energy (E_{dim}, kcal/mol) does not take into account the nuclear relaxation (i.e., it is the difference in energy between the absolute energy of the minimum and the energies of the monomers with the geometry they have at the dimer minimum). Both energies are single-point-corrected for BSSE using the CP correction (E_{int} + CP, and E_{dim} + CP). $R_{H\cdots B}$ stands for the intermolecular distance, whereas $\rho(r_{bcp})$ and $\nabla^2\rho(r_{bcp})$ are the electron densities and their Laplacians at the bond critical point. Two of the main three curvatures at the bond critical point are collected as λ_1 and λ_3, the latter being parallel to the bond. Kinetic ($G(r_{bcp})$) and potential energy ($V(r_{bcp})$) densities at the bcp are also reported.

The rest of this section is split into two parts. In the first one, the behavior of topological and energetic properties as an intermolecular distance function will be analyzed; in the second part, the same analysis will be considered but this time as a function of the hydrogen bond energy formation.

TABLE 1: B3LYP/6-31++G(d,p) CP-Corrected Interaction and CP-Corrected Dimerization Energies (in kcal/mol), Intermolecular Distances (in Å), Electron Density Topological Properties at the Bond Critical Point r_{bcp} (in eÅ^{-3} and eÅ^{-5}), along with Kinetic (*G*) and Potential (*V*) Energy Density Properties (a.u.)

	E_{int} + CP	E_{dim} + CP	$R_{H\cdots B}$	$\rho(r_{bcp})$	$\nabla^2\rho(r_{bcp})$	λ_1	λ_3	$G(r_{bcp})$	$V(r_{bcp})$
NH_3−HF	−14.02	−15.18	1.644	0.059	0.114	−0.111	0.335	0.0372	−0.0460
NH_3−H Cl	−9.66	−11.27	1.683	0.058	0.102	−0.101	0.303	0.0317	−0.0381
NH_3−HBr	−8.40	−12.26	1.543	0.083	0.073	−0.174	0.420	0.0425	−0.0667
H_2O−HF	−9.37	−9.69	1.673	0.044	0.139	−0.076	0.288	0.0335	−0.0322
H_2CO−HF	−8.25	−8.59	1.699	0.042	0.130	−0.071	0.271	0.0313	−0.0302
H_2O−HCl	−5.78	−5.96	1.840	0.033	0.088	−0.046	0.178	0.0219	−0.0218
H_2O−HBr	−4.73	−4.87	1.895	0.030	0.077	−0.041	0.156	0.0198	−0.0204
PH_3−HF	−5.48	−5.88	2.304	0.024	0.037	−0.027	0.091	0.0106	−0.0121
H_2S−HF	−5.46	−5.62	2.250	0.025	0.046	−0.029	0.104	0.0124	−0.0133
H_2CO−HCl	−4.92	−5.12	1.875	0.031	0.079	−0.043	0.164	0.0201	−0.0206
H_2CO−HBr	−4.64	−4.09	1.926	0.029	0.071	−0.040	0.150	0.0188	−0.0199
HF−HF	−4.38	−4.80	1.808	0.026	0.093	−0.040	0.170	0.0225	−0.0217
HBr−HF	−2.70	−2.73	2.447	0.016	0.038	−0.017	0.071	0.0088	−0.0082
PH_3−HCl	−3.24	−3.48	2.476	0.019	0.031	−0.019	0.070	0.0087	−0.0095
H_2S−HCl	−3.21	−3.33	2.420	0.020	0.037	−0.021	0.079	0.0098	−0.0103
HBr−HCl	−1.33	−1.35	2.593	0.014	0.033	−0.014	0.059	0.0076	−0.0070
HBr−HBr	−0.94	−0.95	2.648	0.013	0.032	−0.012	0.055	0.0071	−0.0062
H_2S−HBr	−2.55	−2.64	2.478	0.018	0.037	−0.018	0.074	0.0093	−0.0093
PH_3−HBr	−2.50	−2.70	2.511	0.018	0.033	−0.018	0.069	0.0086	−0.0090
HF−HCl	−2.73	−2.74	2.024	0.018	0.054	−0.024	0.100	0.0144	−0.0153
HCl−HF	−2.71	−2.74	2.348	0.016	0.044	−0.018	0.079	0.0100	−0.0090
HF−HBr	−2.16	−2.16	2.115	0.015	0.048	−0.019	0.085	0.0124	−0.0127
HCl−HCl	−1.44	−1.44	2.583	0.011	0.032	−0.011	0.054	0.0070	−0.0060
HCl−HBr	−1.06	−1.06	2.664	0.010	0.030	−0.009	0.048	0.0062	−0.0049
NaH−HBr	−17.78	−43.69	0.881	0.174	−0.488	−0.520	0.551	0.0206	−0.1634
LiH−HBr	−13.26	−27.02	0.982	0.130	−0.208	−0.339	0.470	0.0252	−0.1023
NaH−HF	−15.02	−16.57	1.328	0.051	0.025	−0.088	0.201	0.0192	−0.0321
NaH−HCl	−14.58	−32.91	0.963	0.138	−0.251	−0.365	0.479	0.0244	−0.1115
LiH−HF	−14.53	−15.75	1.347	0.047	0.033	−0.080	0.193	0.0188	−0.0294
LiH−HCl	−12.37	−17.45	1.176	0.078	−0.022	−0.157	0.291	0.0224	−0.0502
HBeH−HF	−3.85	−3.95	1.594	0.024	0.048	−0.034	0.114	0.0127	−0.0133
HBeH−HBr	−1.51	−1.54	1.788	0.017	0.037	−0.021	0.078	0.0093	−0.0095
HBeH−HCl	−2.01	−2.05	1.786	0.017	0.035	−0.020	0.075	0.0089	−0.0092
H_2BH−HF	−1.58	−1.63	1.886	0.013	0.037	−0.015	0.064	0.0080	−0.0067
H_2BH−HBr	−0.28	−0.28	2.354	0.007	0.024	−0.007	0.033	0.0047	−0.0035
H_2BH−HCl	−0.60	−0.62	2.160	0.008	0.025	−0.008	0.040	0.0051	−0.0038

A. Dependence on Optimized (equilibrium) Intermolecular Distances. Figure 1 plots electron density values at the bond critical point $\rho(r_{bcp})$ vs the hydrogen or dihydrogen optimized bond length ($R_{H\cdots B}$) at B3LYP/6-31++G(d,p) (solid lines) and MP2/6-31++G(d,p) (dash lines). For both sets of systems (HB and DHB) and both levels of calculation, $\rho(r_{bcp})$ shows a typical exponential behavior with the intermolecular distance. No meaningful differences between the results in Tables 1 and 2 are observed. In general, at the MP2 level the interaction between monomers exhibits lower $\rho(r_{bcp})$ than B3LYP calculations. Analysis of both set of complexes reveals clearly that DHB systems have smaller $\rho(r_{bcp})$ as compared to HB dimers. This general trend is found for all systems, ranging from the weakest to the strongest ones. Since all dihydrogen-bonded systems consist of the same proton acceptor (a hydrogen atom), the change of its $\rho(r_{bcp})$ with the intermolecular distance is much more homogeneous ($R^2 = 0.999$) than it is for hydrogen-bonded systems ($R^2 = 0.936$ and 0.870 for B3LYP and MP2, respectively), where different proton acceptors are considered.

Some authors have classified[5,13] interaction energies by means of $\nabla^2\rho(r_{bcp})$. It is well-known that not only $\rho(r_{bcp})$ is interesting to be analyzed, but also the way that this electronic charge density is distributed around the intermolecular region. The sign of the Laplacian will determine if the electronic charge is locally concentrated ($\nabla^2\rho(r_{bcp}) < 0$) or depleted ($\nabla^2\rho(r_{bcp}) > 0$). Figure 2 plots $\nabla^2\rho(r_{bcp})$ vs equilibrium $R_{H\cdots B}$ for this purpose.

The discussion of Figure 2 can be focused on two different aspects: first, the comparison between HB and DHB $\nabla^2\rho(r_{bcp})$, and second, the observed change of Laplacian sign. Regarding topological differences between both intermolecular bonds (HB and DHB), it can be seen that DHB display lower Laplacian values than HB complexes. The different electronic structure of the atoms involved in the intermolecular interactions will bring about a different behavior when the classification is based merely on $\rho(r_{bcp})$ values. This is the main reason that DHB systems have a smaller $\rho(r_{bcp})$ than HB systems.

A more interesting analysis can be carried out by checking the sign of Laplacian values. It is well-known that positive values indicate a closed-shell interaction, while negative values correspond to shared-shell interactions. All studied hydrogen-bonded complexes exhibit a positive value of the Laplacian, thus indicating a depletion of the charge. This fact, along with the low values of $\rho(r_{bcp})$, allows classifying the HB interaction as closed-shell. On the contrary, for dihydrogen-bonded systems both positive and negative values of the Laplacian are found—the stronger complexes having the most negative values. This behavior was already found in earlier studies for very strong hydrogen and dihydrogen bonds.[17,18] Likewise, the trend of Laplacian as a function of distance is in very good agreement with previous studies.[13,14] Starting from large intermolecular distances (pure closed-shell systems), there is a smooth increase of $\nabla^2\rho(r_{bcp})$ while shortening the bond—the Laplacian value reaching a maximum; from this point, $\nabla^2\rho(r_{bcp})$ starts decreasing along with the distance, being very steep when the Laplacian becomes negative. Interestingly, the largest difference between MP2 and B3LYP results can be found for very short intermolecular distances.

TABLE 2: MP2/6-31++G(d,p) CP-Corrected Interaction and CP-Corrected Dimerization Energies (in kcal/mol), Intermolecular Distances (in Å), Electron Density Topological Properties at the Bond Critical Point r_{bcp} (in eÅ^{-3} and eÅ^{-5}), along with Kinetic (G) and Potential (V) Energy Density Properties (a.u.)

	E_{int} + CP	E_{dim} + CP	$R_{H\cdots B}$	$\rho(r_{bcp})$	$\nabla^2\rho(r_{bcp})$	λ_1	λ_3	$G(r_{bcp})$	$V(r_{bcp})$
NH_3−HF	−12.05	−12.92	1.673	0.050	0.131	−0.091	0.313	0.037	−0.041
NH_3−HCl	−7.18	−7.79	1.817	0.040	0.098	−0.058	0.213	0.025	−0.025
NH_3−HBr	−6.60	−7.91	1.717	0.051	0.106	−0.085	0.276	0.031	−0.035
H_2O−HF	−8.22	−8.43	1.716	0.035	0.141	−0.057	0.252	0.031	−0.027
H_2CO−HF	−7.23	−7.48	1.743	0.034	0.133	−0.054	0.240	0.030	−0.026
H_2O−HCl	−4.91	−5.00	1.903	0.026	0.079	−0.034	0.146	0.020	−0.019
H_2O−HBr	−4.49	−4.56	1.951	0.024	0.072	−0.031	0.131	0.018	−0.018
PH_3−HF	−4.44	−4.67	2.346	0.021	0.042	−0.022	0.085	0.010	−0.010
H_2S−HF	−4.06	−4.14	2.298	0.020	0.049	−0.022	0.093	0.011	−0.011
H_2CO−HCl	−4.25	−4.36	1.936	0.026	0.074	−0.033	0.139	0.019	−0.019
H_2CO−HBr	−3.83	−3.95	1.974	0.025	0.070	−0.032	0.132	0.018	−0.019
HF−HF	−4.21	−4.23	1.858	0.020	0.090	−0.029	0.147	0.020	−0.018
HBr−HF	−2.14	−2.16	2.534	0.012	0.033	−0.012	0.056	0.007	−0.006
PH_3−HCl	−2.43	−2.51	2.586	0.015	0.029	−0.014	0.058	0.007	−0.008
H_2S−HCl	−2.19	−2.21	2.528	0.015	0.034	−0.015	0.062	0.008	−0.008
HBr−HCl	−0.99	−1.00	2.666	0.012	0.029	−0.011	0.050	0.007	−0.006
HBr−HBr	−1.08	−1.09	2.704	0.011	0.029	−0.010	0.048	0.007	−0.006
H_2S−HBr	−2.00	−2.02	2.559	0.014	0.035	−0.014	0.062	0.008	−0.008
PH_3−HBr	−2.18	−2.26	2.582	0.016	0.032	−0.015	0.061	0.008	−0.008
HF−HCl	−2.43	−2.43	2.065	0.016	0.052	−0.019	0.090	0.013	−0.014
HCl−HF	−2.01	−2.03	2.377	0.013	0.043	−0.014	0.071	0.009	−0.008
HF−HBr	−0.68	−0.70	2.143	0.013	0.048	−0.016	0.079	0.012	−0.012
HCl−HCl	−1.11	−1.11	2.603	0.010	0.031	−0.010	0.050	0.007	−0.006
HCl−HBr	−1.12	−1.13	2.648	0.010	0.030	−0.009	0.048	0.007	−0.005
NaH−HBr	−17.18	−54.65	0.832	0.198	−0.771	−0.631	0.491	0.015	−0.222
LiH−HBr	−10.01	−28.52	0.935	0.143	−0.339	−0.396	0.453	0.024	−0.133
NaH−HF	−14.08	−15.44	1.349	0.045	0.045	−0.074	0.192	0.020	−0.029
NaH−HCl	−10.07	−26.13	0.992	0.123	−0.219	−0.312	0.405	0.025	−0.105
LiH−HF	−12.85	−13.78	1.383	0.040	0.052	−0.063	0.177	0.019	−0.025
LiH−HCl	−8.83	−9.98	1.420	0.041	0.036	−0.061	0.158	0.016	−0.024
HBeH−HF	−2.93	−2.98	1.694	0.018	0.046	−0.022	0.088	0.010	−0.009
HBeH−HBr	−1.38	−1.39	1.963	0.008	0.030	−0.008	0.039	0.005	−0.004
HBeH−HCl	−1.63	−1.63	1.974	0.011	0.028	−0.011	0.050	0.006	−0.006
H_2BH−HF	−0.76	−0.80	2.041	0.007	0.023	−0.008	0.038	0.005	−0.004
H_2BH−HBr	0.03	0.02	2.584	0.006	0.021	−0.006	0.028	0.004	−0.003
H_2BH−HCl	−0.46	−0.47	2.138	0.007	0.021	−0.007	0.036	0.005	−0.004

To get a deeper insight on the different behavior of the $\nabla^2\rho(r_{bcp})$ in HB and DHB systems, we have decomposed the Laplacian into its three curvatures: λ_1 and λ_2 (negative curvatures perpendicular to the bond) and λ_3 (positive parallel curvature), and analyzed them independently. The curvatures perpendicular to the bond (λ_1, λ_2) will be discussed together, as they have a similar value due to the cylindrical symmetry of the bond.

In Figure 3 we plot λ_1 and λ_3 as a function of the intermolecular distance, $R_{H\cdots B}$. It can be noted that the dependence of curvature vs bond length is again more homogeneous for DHB systems than for HB complexes for both the MP2 and B3LYP levels of theory (i.e., at the MP2 level of theory $R^2 = 0.9997$ for DHB/λ_1 while $R^2 = 0.926$ for HB/λ_1). At large distances of DHB systems, λ_3 is more sensitive than λ_1 to the decrease of the equilibrium bond length, as compared with the corresponding decrease in HB complexes. The fact that the variation of λ_3 values vs λ_1 values is more noticeable in HB complexes is the reason for the decrease in the Laplacian values of DHB complexes (recall that the Laplacian is calculated as the sum of the three curvatures). For both curvatures, DHB values are always much lower, exhibiting larger differences as the intermolecular distance becomes shorter. It is worth mentioning that these curvatures show a very well-defined trend versus intermolecular distances, which is in very good agreement with earlier works where the positive curvature was found to be the most meaningful parameter for hydrogen bond characterization and classification.[9]

Among all topological characteristics that can be considered, the energetic properties of $\rho(r)$ at the bond critical point are a good representation of the intermolecular interaction. In this scope we proceed to discuss the HB and DHB systems in terms of energy component densities, that is, kinetic and potential energies ($G(r_{bcp})$ and $V(r_{bcp})$). Thus, in Figure 4 the relation between $G(r_{bcp})$ and $V(r_{bcp})$ with the intermolecular distance is plotted at the B3LYP/6-31++G(d,p) and MP2/6-31++G(d,p) levels of theory. As Espinosa et al. showed,[8] for closed-shell systems there is a linear relationship between $G(r_{bcp})$ and λ_3, while $V(r_{bcp})$ is linearly related to the sum of the other two curvatures ($\lambda_1 + \lambda_2$). Having this fact in mind, at large intermolecular distances, Figure 4 shows a shape similar to that in Figure 3. $G(r_{bcp})$ can be interpreted as a contribution of the electron dilution involved in the bond formation. As pointed out above, DHB systems display $\rho(r_{bcp})$ as well as lower concentration/depletion of this electron density. This fact is in full agreement with the lower value of $G(r_{bcp})$ shown by DHB complexes. There is also a decrease of DHB $V(r_{bcp})$ as compared to HB dimers. In that way, a lower $\rho(r_{bcp})$ is related to $V(r_{bcp})$, due to weaker capacity to accumulate electrons. Once again, there is a similar behavior for both MP2 and B3LYP levels of calculation.

A second point to be considered here concerns the distance shortening and $\nabla^2\rho(r_{bcp})$ becoming negative. While λ_3 keeps increasing when shortening the distance (see Figure 3), $G(r_{bcp})$ presents a maximum for DHB with a final decrease for NaH···HBr; this is actually the complex with the shortest intermolecular distance. Espinosa et al.[13] had already found this behavior for XH···FY, hence classifying the shorter distance complexes as shared-shell interactions.

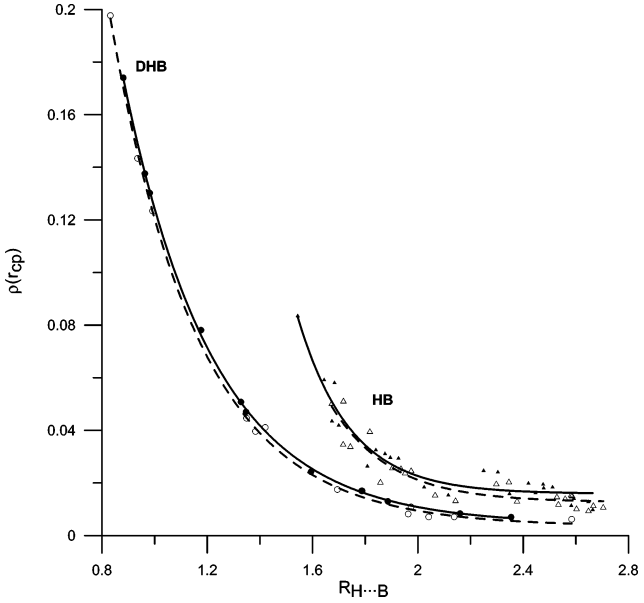

Figure 1. Electron density at the bond critical point (e•Å^{-3}) versus intermolecular distance (Å). Solid circles and triangles are for B3LYP calculations (DHB and HB, respectively), the solid lines being their fitted curves. Empty circles and triangles are for MP2 calculations (DHB and HB, respectively), the dashed lines being their fitted curves.

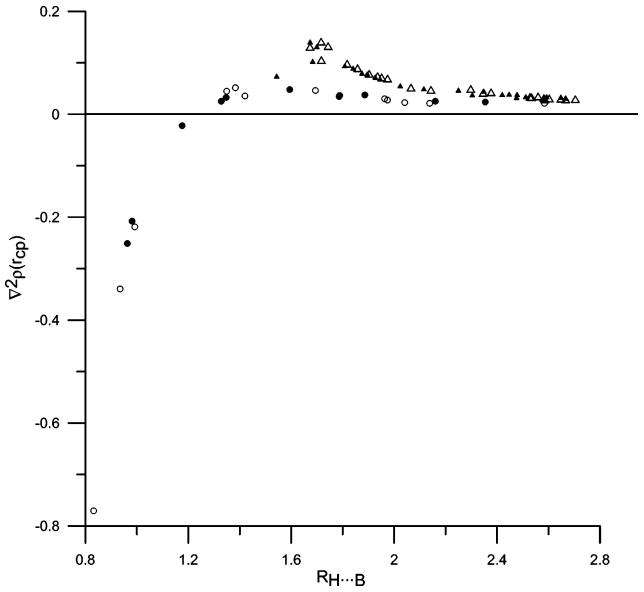

Figure 2. Laplacian of the electron density at the bond critical point (e•Å^{-5}) versus the intermolecular distance (Å). Solid circles and triangles are for B3LYP calculations (DHB and HB, respectively), while empty circles and triangles are for MP2 (DHB and HB, respectively).

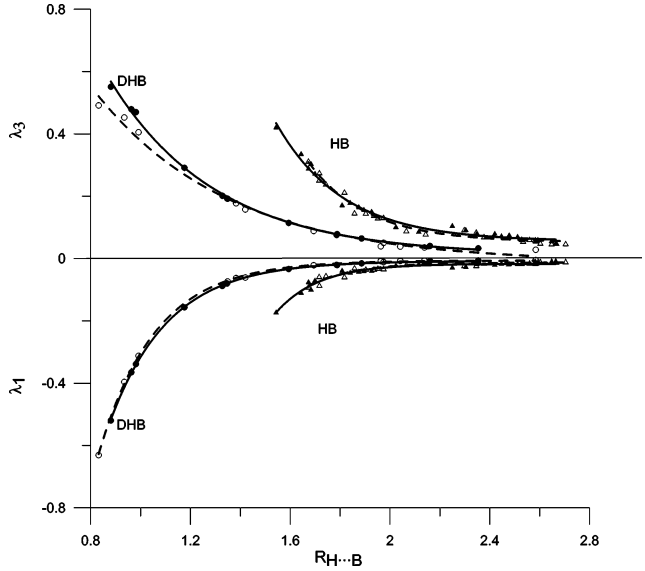

Figure 3. λ_1 and λ_3 (e•Å^{-5}) at the bond critical point versus the intermolecular distance (Å). Solid circles and triangles are for B3LYP calculations (DHB and HB, respectively), the solid lines being their fitted curves. Empty circles and triangles are for MP2 calculations (DHB and HB, respectively), the dashed lines being their fitted curves.

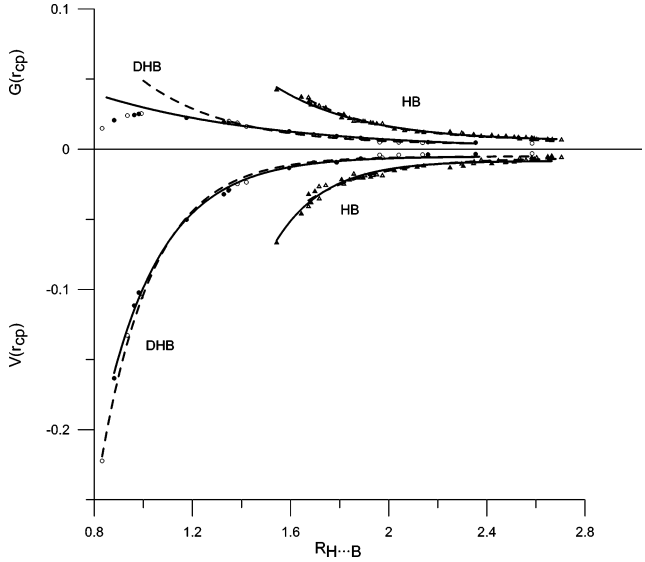

Figure 4. Potential ($V(r_{bcp})$) and kinetic ($G(r_{bcp})$) energy densities (a.u.) at the bond critical point versus the intermolecular distance (Å). Solid circles and triangles are for B3LYP calculations (DHB and HB, respectively), the solid lines being their fitted curves. Empty circles and triangles are for MP2 calculations (DHB and HB, respectively), the dashed lines being their fitted curves.

For complexes characterized as closed-shell, we can obtain a very appealing separation between HB and DHB systems (Figure 4). Note that the correlation between $G(r_{bcp})$ and $R_{H\cdots B}$ is very good at both levels of theory and all systems ($R^2 = 0.988$ for DHB/MP2 and $R^2 = 0.992$ for the others).

B. HB/DHB Strength Dependence.

So far, the characterization of dihydrogen-bonded systems has been analyzed in terms of intermolecular distances ($R_{H\cdots B}$). However, another usual attractive point of view can be considered in terms of strength, that is, considering the energy implied in the formation of DHB.

Figure 5 shows how the CP-corrected dimerization energy (with no nuclear relaxation) correlates with intermolecular distance. As found in previous studies,[10] there is an exponential relationship between geometrical parameters ($R_{H\cdots B}$) and the interaction strength (E_{dim} + CP). Figure 5 shows how DHB complexes with dimerization energy similar to HB systems present shorter distances. Since in the first part of this section we concluded that, in general, DHB have lower $\rho(r_{bcp})$ and also a lower curvature, the present conclusion fully agrees with the fact that DHB are weaker at the same interatomic distance. A common behavior is found for the B3LYP and MP2 levels of theory. It must be noted that the NH_3-HBr complex presents a $R_{H\cdots B}$ distance (1.543 Å) which is too short compared to complexes of similar dimerization energy. The reason may be found in its very large BSSE (2.45 kcal/mol estimated by CP). In a previous paper,[19] it was showed that there is a linear relationship between the amount of CP correction to the energy

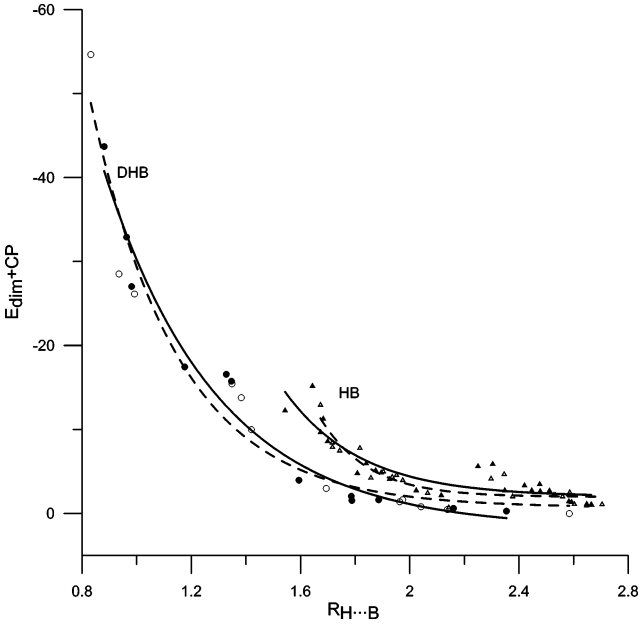

Figure 5. BSSE-corrected dimerization energy (kcal/mol) versus intermolecular distance (Å). Solid circles and triangles are for B3LYP calculations (DHB and HB, respectively), the solid lines being their fitted curves. Empty circles and triangles are for MP2 calculations (DHB and HB, respectively), the dashed lines being their fitted curves.

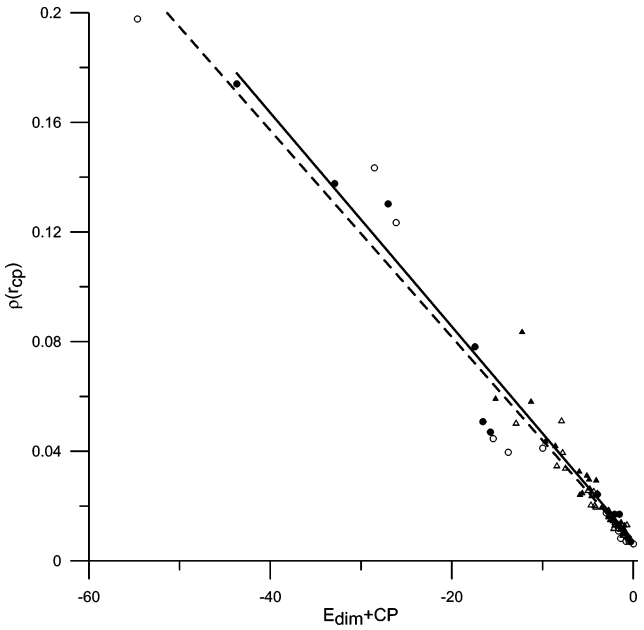

Figure 6. Electron density at the bond critical point (e•Å^{-3}) versus dimerization energy (kcal/mol). Solid circles and triangles are for B3LYP calculations (DHB and HB, respectively), the solid line being their fitted curve. Empty circles and triangles are for MP2 calculations (DHB and HB, respectively), the dashed line being their fitted curve.

and the change in the intermolecular distance if the geometry is reoptimized using the CP-corrected scheme. In this particular case, reoptimizing in a CP-corrected surface would increase the NH_3-HBr distance and thus improve the correlation with that of others complexes.

As a result of the trend shown in Figure 5, it was interesting to reanalyze the topology of the HB/DHB interactions and energy density values $V(r)$ and $G(r)$ at the bond critical point as a function of the energetic criteria. Therefore, we plotted (Figure 6) $\rho(r_{bcp})$ as a function of the dimerization energy (E_{dim} + CP). Comparing this graphic with 1 (electron density represented as a function of $R_{H\cdots B}$), it can readily be observed

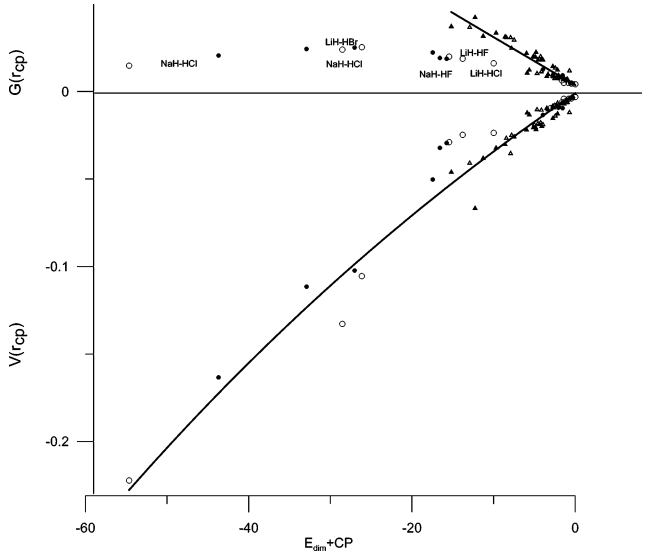

Figure 7. Potential ($V(r_{bcp})$) and kinetic ($G(r_{bcp})$) energy densities (a.u.) at the bond critical point versus the dimerization energy (kcal/mol). Solid circles and triangles are for B3LYP calculations (DHB and HB, respectively), and empty circles and triangles are for MP2 calculations (DHB and HB, respectively). Solid lines correspond to fitted curves for all MP2 and B3LYP data together. For $G(r_{bcp})$, only purely closed-shell data are considered in the fitted data.

that there is no actual, clear separation between HB and DHB systems. Furthermore, comparing the solid line (B3LYP data) with the dashed line (MP2 data), one can assess again that no significant differences are observed, as far as topological behavior is concerned. A similar behavior is observed by plotting the Laplacian ($\nabla^2\rho(r_{bcp})$) or the two curvatures λ_1 and λ_3 vs E_{dim}.

To further assess the relationship between density topological parameters and energetic data, we proceed to a final analysis of the kinetic and potential energy densities at r_{bcp}. Because of the linear relationship existing for closed-shell interactions between the curvatures ($\lambda_1 + \lambda_2$ and λ_3) at the bcp and $V(r_{bcp})$ and $G(r_{bcp})$, respectively, we might expect from Figure 7 that no significant differences will be found between HB and DHB when energy densities are analyzed. This fact can be verified in Figure 7, where $G(r_{bcp})$ and $V(r_{bcp})$ are represented vs the dimerization energy. If we focus on the systems with larger intermolecular distances, there is no actual difference between HB and DHB. However, when the distance decreases there is a maximum in $G(r_{bcp})$. Espinosa et al.[13] claimed that this fact (the increase and further decrease of $G(r_{bcp})$ while shortening the intermolecular distance) is related to the covalent contribution to the bond. Comparing Figure 7 and Figure 4 ($G(r_{bcp})$ versus $R_{H\cdots X}$ and CP-corrected dimerization energy, respectively), one can observe that, for DHB complexes, all MH···HX (M = Na, Li) systems deviate significantly from the HB set. As mentioned above, all these systems have very short intermolecular distances, which can be translated into an important covalent contribution. In that way, the representation of $G(r_{bcp})$ versus dimerization energies assess in a better way the separation between closed-shell and shared-shell systems.

The results presented so far show that hydrogen- and dihydrogen-bonded systems have topological and energetic properties which show a similar dependence with intermolecular strength, that is, with dimerization energies.[7,16] This fact is in complete agreement with previous studies which found a similar behavior for HB and DHB. The present study evidence that, on the contrary, when the intermolecular distance is considered, meaningful differences can be found between the set of HB or

DHB complexes; such differences, induced by lower density and concentration/depletion electron charge density, allow for a remarkable separation of both sets of intermolecular bonds and thus provide a nice way for their classification. Overall, they provide a neater way to understand HB and DHB systems, which enhances earlier studies.

The present work will be extended in the near future to geometries and densities obtained for CP-corrected surfaces, and will be the subject of another paper.

IV. Conclusions

B3LYP/6-31++G(d,p) and MP2/6-31++G(d,p) calculations for various different hydrogen-bond and dihydrogen-bond systems have been carried out in order to analyze their electron density topological and local energetic properties at the bond critical point at the optimized geometries. MP2 and B3LYP topological and energetic data give rise to very similar conclusions. Both levels of calculations predict the same topological differences between HB and DHB complexes.

H···H interactions exhibit shorter dihydrogen bond lengths as compared with hydrogen-bonded systems with the same strength. This behavior can be rationalized from the lower $\rho(r_{bcp})$, as well as a lower concentration/depletion of that density, which is due to the different electronic structure of both atoms taking part in the interaction.

While there are no significant differences when properties are represented as a function of the dimerization energy, they can be separated into two well-defined sets when intermolecular hydrogen bond distances are considered.

For dihydrogen-bonded complexes it can be observed that their trends are more homogeneous, due to both atoms involved in the intermolecular interaction being the same in all complexes. Ranging from very weak to very strong dihydrogen-bonded complexes, we have found that results for the topological and energetic values of $\rho(r_{bcp})$ are similar to those found earlier for density by Espinosa et al. for XH···FY complexes, thus revealing important covalent contribution for very strong systems.

All in all, we have characterized the relationship between $\rho(r_{bcp})$ properties and intermolecular distances; this relationship is different for the set of dihydrogen-bonded systems and for the set of other standard hydrogen-bond complexes. Thus we have been able to assess the differences between these two types of systems and to stress the importance of taking into account hydrogen-bond-optimized equilibrium distances instead of energetic (i.e., dimerization energies) values. The latter parameters do not give rise to a classification and separation of both sets of hydrogen-bonded systems. Plotting against bond length does, and hence it allows for better understanding of the different properties of HB and DHB complexes.

Acknowledgment. Financial help has been furnished by the Spanish Ministerio de Educación y Ciencia (MEC) Projects CTQ2005-08797-C02-01/BQU and CTQ2005-02698, and also by the Departament d'Universitats, Recerca i Societat de la Informació (DURSI) Project No. 2005SGR-00238. D.H. thanks the Spanish MCYT for the benefit from a doctoral fellowship.

Supporting Information Available: Equilibrium geometries at the B3LYP/6-31++G(d,p) and MP2/6-31++G(d,p) (Table S.1) levels of theory and correlation for graphics in Figures 1−7 (Table S.2). This material is available free of charge at http://pubs.acs.org.

References and Notes

(1) (a) Jeffrey, G. A. *An Introduction to Hydrogen Bonding*; Oxford University Press: New York, 1997. (b) Scheiner, S. *An Introduction to Hydrogen Bonding*; Oxford University Press: New York, 1997. (c) Desiraju, G. R.; Steiner, T. *The Weak Hydrogen Bond*; Oxford University Press: New York, 1999. (d) Steiner, T. *Angew. Chem. Int. Ed.* **2002**, *41*, 48.

(2) Crabtree, R. H.; Siegbahn, P. E. M.; Eisenstein, O.; Rheingold, A. L.; Koetzle, T. F. *Acc. Chem. Res.* **1996**, *29*, 348, and references therein.

(3) (a) Bakhmutov, V. I. *Eur. J. Inorg. Chem.* **2005**, *2*, 245. (b) Epstein, L. M.; Shubina, E. S. *Coord. Chem. Rev.* **2002**, *231*, 165. (c) Custelcean, R.; Jackson, J. E. *Chem. Rev.* **2001**, *101*, 1963. (d) Maseres, F.; Lledós. A.; Clot, E.; Eisenstein, O. *Chem. Rev.* **2000**, *100*, 601.

(4) (a) Robertson, K. N.; Knop, O.; Cameron, T. S. *Can. J. Chem.* **2003**, *81*, 727. (b) Matta, C. F.; Hernández-Trujillo, J; Tang, T. H.; Bader, R. F. W. *Chem. Eur. J.* **2003**, *9*, 1940. (c) Hugas, D.; Simon, S.; Duran, M. *Chem. Phys. Lett.* **2004**, *386*, 373. (d) Remko, M. *Mol. Phys.* **1998**, 94, 839. (e) Grabowski, S. J. *J. Mol. Struct.* **2000**, *553*, 151. (f) Grabowski, S. J. *J. Phys. Chem. A* **2000**, *104*, 5551. (g) Kulkarni, S. A.; Srivastava, A. K. *J. Phys. Chem. A* **1999**, *103*, 2836. (h) Kulkarni, S. A. *J. Phys. Chem. A* **1998**, *102*, 7704. (i) Alkorta, I.; Rozas, I.; Elguero, J. *Chem. Soc. Rev.* **1998**, *27*, 163.

(5) Bader, R. F. W. *Atoms in Molecules: A Quantum Theory*; Oxford University Press: Oxford, 1990.

(6) Koch, U.; Popelier, P. L. A. *J. Phys. Chem.* **1995**, *99*, 9747.

(7) Popelier, P. L. A. *J. Phys. Chem. A* **1998**, *102*,1873.

(8) (a) Espinosa, E.; Lecomte, C.; Molins, E. *Chem. Phys. Lett.* **1998**, *285*, 170. (b) Espinosa, E.; Lecomte, C.; Molins, E. *Chem. Phys. Lett.* **1999**, *300*, 745. (c) Espinosa, E.; Alkorta, I.; Rozas, I.; Elguero, J.; Molins, E. *Chem. Phys. Lett.* **2001**, *336*, 457.

(9) Espinosa, E.; Souhassou, M.; Lachekar, H.; Lecomte, C. *Acta Crystallogr.* **1999**, *B55*, 563.

(10) Grabowski, S. J. *J. Phys. Org. Chem.* **2004**, *17*, 18.

(11) (a) Grabowski, S. J. *J. Phys. Chem. A* **2001**, *105*, 10739. (b) Grabowski, S. J. *Chem. Phys. Lett.* **2001**, *338*, 361. (c) Grabowski, S. J. *J. Mol. Struct.* **2001**, *562*, 137.

(12) (a) Fuster, F.; Silvi, B. *Theor. Chem. Acc.* **2001**, *104*, 13. (b) Fuster, F.; Silvi, B.; Berski, S.; Latajka, Z. *J. Mol. Struct. (Theochem)* **2000**, *555*, 75.

(13) Espinosa, E.; Alkorta, I.; Elguero, J.; Molins, E. *J. Chem. Phys.* **2002**, *117*, 5529.

(14) Gálvez, O.; Gómez, P. C.; Pacios, L. F. *J. Chem. Phys.* **2001**, *115*, 11166.

(15) Pacios, L. F. *J. Phys. Chem. A* **2004**, *108*, 1177.

(16) Grabowski, S. J. *Chem. Phys. Lett.* **1999**, *312*, 542.

(17) (a) Grabowski, S. J.; Sokaldi, W. A.; Leszczynski, J. *J. Phys. Chem. A* **2004**, *108*, 5823. (b) Lipwoski, P.; Grabowski, S. J.; Robinson, T. L.; Leszczynski, J. *J. Phys. Chem. A* **2004**, *108*, 10865. (c) Merino, G.; Bakhmutov, V. I.; Vela, V. *J. Phys. Chem. A* **2002**, *106*, 8491. (d) Alkorta, I.; Elguero, J.; Mó, O.; Yañez, M.; Del Bene, J. E. *J. Phys. Chem. A* **2002**, *106*, 9325. (e) Kar, T.; Scheiner, S. *J. Chem. Phys.* **2003**, *119*, 1473.

(18) Hugas, D.; Simon, S.; Duran, M. *Struct. Chem.* **2005**, *16*, 257.

(19) (a) Simon, S.; Bertran, J.; Sodupe, M. *J. Phys. Chem. A* **2001**, *105*, 4359. (b) Poater, J.; Fradera, X.; Solà, M.; Duran, M.; Simon, S. **2003**, *369*, 248.

(20) (a) Grabowski, S. J.; Robinson, T. L.; Leszczynski, J. *Chem. Phys. Lett.* **2004**, *386*, 44. (b) Grabowski, S. J.; Sokalski, W. A.; Leszczynski, J. *J. Phys. Chem. A* **2005**, *109*, 4331.

(21) Wolstenholme, D. J.; Cameron, T. S. *J. Phys. Chem. A* **2006**, *110*, 8970.

(22) (a) Becke, A. D. *J. Chem. Phys.* **1993**, *98*, 5648. (b) Lee, C.; Yang, W.; Parr, R. G. *Phys. Rev. B* **1988**, *37*, 785.

(23) Salvador, S.; Paizs, B.; Duran, M.; Suhai, S. *J. Comput. Chem.* **2001**, *22*, 765.

(24) Boys, S. F.; Bernardi, F. *Mol. Phys.* **1970**, *19*, 553.

(25) Frisch, M. J.; Trucks, G. W.; Schlegel, H. B.; Scuseria, G. E.; Robb, M. A.; Cheeseman, J. R.; Zakrzewski, V. G.; Montgomery, J. A.; Stratmann, R. E.; Burant, J. C.; Dapprich, S.; Millam, J. M.; Daniels, A. D.; Kudin, K. N.; Strain, M. C.; Farkas, O.; Tomasi, J.; Barone, V.; Cossi, M.; Cammi, R.; Mennucci, B.; Pomelli, C.; Adamo, C.; Clifford, S.; Ochterski, J.; Petersson, G. A.; Ayala, P. Y.; Cui, Q.; Morokuma, K.; Malick, D. K.; Rabuck, A. D.; Raghavachari, K.; Foresman, J. B.; Cioslowski, J.; Ortiz, J. V.; Stefanov, B. B.; Liu, G.; Liashenko, A.; Piskorz, P.; Komaromi, I.; Gomperts, R.; Martin, L. R.; Fox, D. J.; Keith, T.; Al-Laham, M. A.; Peng, C. Y.; Nanayakkara, A.; Gonzalez, G.; Challacombe, M.; Gill, P. M. W.; Johnson, B.; Chen, W.; Wong, M. W.; Andres, J. L.; Gonzalez, C.; Head-Gordon, M.; Replogle, E. S.; Pople, J. A. *Gaussian 03*, Rev. C.02; Gaussian, Inc.: Wallingford, CT, 2004.

(26) AIM2000 designed by F. Biegler-König, University of Applied Science, Bielefeld, Germany.